

Cite this: *Nanoscale*, 2011, **3**, 1421

www.rsc.org/nanoscale

## FEATURE ARTICLE

## Gold nanoparticles for the colorimetric and fluorescent detection of ions and small organic molecules

Dingbin Liu,<sup>ab</sup> Zhuo Wang<sup>\*a</sup> and Xingyu Jiang<sup>\*a</sup>

Received 19th November 2010, Accepted 7th January 2011

DOI: 10.1039/c0nr00887g

In recent years, gold nanoparticles (AuNPs) have drawn considerable research attention in the fields of catalysis, drug delivery, imaging, diagnostics, therapy and biosensors due to their unique optical and electronic properties. In this review, we summarized recent advances in the development of AuNP-based colorimetric and fluorescent assays for ions including cations (such as  $\text{Hg}^{2+}$ ,  $\text{Cu}^{2+}$ ,  $\text{Pb}^{2+}$ ,  $\text{As}^{3+}$ ,  $\text{Ca}^{2+}$ ,  $\text{Al}^{3+}$ , etc) and anions (such as  $\text{NO}_2^-$ ,  $\text{CN}^-$ ,  $\text{PF}_6^-$ ,  $\text{F}^-$ ,  $\text{I}^-$ , oxoanions), and small organic molecules (such as cysteine, homocysteine, trinitrotoluene, melamine and cocaine, ATP, glucose, dopamine and so forth). Many of these species adversely affect human health and the environment. Moreover, we paid particular attention to AuNP-based colorimetric and fluorescent assays in practical applications.

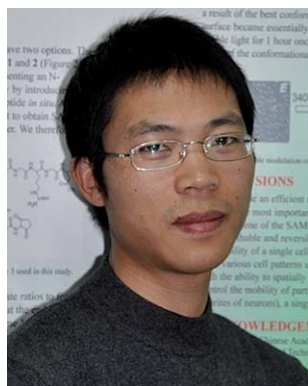
## 1. Introduction

Many aspects of human life depend critically on ensuring the proper levels of ions and small organic molecules that potentially threaten the safety of our environment and food supply. Recent development of analytical chemistry and nanotechnology has provided a toolbox for assaying a variety of targets. Researchers have introduced a large number of assays for both ions and small organic molecules, such as those based on chemical sensors by using organic dyes,<sup>1–3</sup> DNazymes,<sup>4,5</sup> proteins,<sup>6</sup> thin films,<sup>7,8</sup>

polymeric materials,<sup>9</sup> electrochemistry,<sup>10–14</sup> inductively coupled plasma mass spectroscopy (ICP-MS),<sup>15,16</sup> surface plasmon resonance spectroscopy,<sup>17,18</sup> and atomic absorption spectroscopy.<sup>19</sup> Some of these methods have been used to detect specific targets due to their unique advantages such as high sensitivity and availability. However, most of these assays have various limitations with respect to selectivity, cost, simplicity, aqueous solubility and sensitivity. Thus, the development of simple and inexpensive assays for targets is in high demand. Gold nanoparticles (AuNPs), with the size range of 1–100 nm, have recently attracted considerable attention because of their many distinctive physical and optical properties such as surface plasmon resonance (SPR), surface enhanced Raman scattering (SERS), nonlinear optical (NLO) properties and quantized charging effect.<sup>20–25</sup> Indeed, the past few years have witnessed a variety of

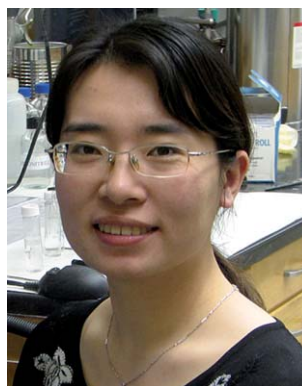
<sup>a</sup>CAS Key Lab for Biological Effects of Nanomaterials and Nanosafety, National Center for Nanoscience and Technology, Beijing, 100190, China. E-mail: xingyujiang@nanoctr.cn; wangz@nanoctr.cn; Fax: (+86)10-82545631; Tel: (+86)10-82545611

<sup>b</sup>Graduate School of Chinese Academy of Sciences, Beijing, 100080, China



Dingbin Liu

Dingbin Liu is currently a PhD candidate at NCNST under the supervision of Prof. Xingyu Jiang. He received his BS from Lanzhou University in 2006 and MS from Chengdu Institute of Biology, Chinese Academy of Sciences in 2009. His current research interest is the design of gold nanoparticles (AuNPs) for ultrasensitive detection of biomolecules. He is also interested in the construction of AuNP-based drug delivery systems.



Zhuo Wang

Zhuo Wang received her MS from the Northeast Normal University (P. R. China) in 2003 and her PhD in Organic Chemistry from the Institute of Chemistry, Chinese Academy of Sciences in 2006. After two years of postdoctoral research at Bowling Green State University (USA), she joined the NCNST as an assistant professor. Her research interests focus on the synthesis and modification of nanoparticles, and the biochemical assays based on small organic molecules and nanomaterials.

AuNP-based sensors in the aspects of electrochemical, SERS, fluorescent and colorimetric assays.<sup>20–27</sup> In particular, AuNP-based colorimetric assays have drawn considerable attention since the pioneering work of using AuNP-based colorimetric assay for DNA detection ten years ago, and then led to an explosive development of colorimetric sensors for species including DNA, proteins, ions and organic molecules.<sup>26</sup> Because there have been many reviews that exclusively described the AuNP-based SERS<sup>20,21</sup> and electrochemical sensors,<sup>22–25</sup> in this critical review we thus mainly describe the AuNP-based colorimetric assays, as well as AuNP-based fluorescent assays that are commonly used to enhance sensitivity.

AuNP-based colorimetric assays are of particular interest because molecular events can be easily transformed into color changes, which can be observed by the naked eye alone, hence, no sophisticated instruments are required. The color change is highly sensitive to the size, shape, capping agents, medium refractive index, as well as the aggregation state of AuNPs.<sup>28</sup> In general, solutions containing well-dispersed AuNPs (normally 10–50 nm in diameter) display a ruby red color while those containing large AuNPs (>50 nm) or aggregates of small AuNPs exhibit a purple or blue color. During the aggregation of AuNPs or dispersion of AuNP aggregates, the color change is associated with the interparticle plasmon coupling that generates a significant absorption band shift in the visible region of the electromagnetic spectrum.<sup>29,30</sup> There are two main kinds of aggregation mechanisms. One is based on the target-triggered removal of stabilizing ligands from surfaces of AuNPs, which is called “non-crosslinking aggregation”, the other is dependent on the binding of ligands modified on AuNPs with target analytes, which is defined as “interparticles crosslinking aggregation”.<sup>31</sup> Owing to their extremely high extinction coefficients (e.g.,  $2.7 \times 10^8 \text{ M}^{-1}\text{cm}^{-1}$  for 13 nm AuNPs), >1000 times higher than those of organic dyes,<sup>29</sup> the limit of detection (LOD) for AuNP-based colorimetric assays can be as low as nM level, which makes this colorimetric sensor widely used in detecting analytes related to diagnosis of diseases, and monitoring environmental contamination and food safety. Since many reviews focused on the colorimetric detection of DNAs and proteins using AuNPs have been provided,<sup>32–36</sup> we therefore attempt to exclusively review recent advances in the development of AuNP-based colorimetric

and fluorescent assays for ions including cations and anions, and small organic compounds.

## 2. Assays for cations

### 2.1 Detection of mercuric ions

Mercury poses severe threats to both human health and the environment.<sup>37</sup>  $\text{Hg}^{2+}$  contaminates water and soil, and transforms into methyl mercury to accumulate in human body through the food chain which may damage many organs.<sup>38–40</sup> The past decade has witnessed a rapid development of assays for  $\text{Hg}^{2+}$  based on AuNPs. According to the aggregation mechanisms, there are two main kinds of AuNP-based assays for  $\text{Hg}^{2+}$ , one is based on “non-crosslinking aggregation”, and the other is dependent on “interparticles crosslinking aggregation”.

The most important example for non-crosslinking aggregation mechanism is based on DNA-conjugated AuNPs (DNA-AuNPs).  $\text{Hg}^{2+}$ -induced abstraction of ligands such as short single-stranded DNA or double-stranded DNA from the surfaces of AuNPs can cause the aggregation of AuNPs, which can be used to detect  $\text{Hg}^{2+}$ .<sup>41–44</sup> Single-stranded DNA, designed to contain thymine-rich (T-rich) domains, can absorb onto the surfaces of unmodified AuNPs. The functionalized AuNPs are monodispersed in aqueous media due to the electrostatic repulsion between the nucleic acid. Upon the addition of  $\text{Hg}^{2+}$ , the complexation of  $\text{Hg}^{2+}$  with T-rich domains yields a hairpin structure, removing the single-stranded DNA from surfaces of AuNPs. The abstraction of ligands from Au surfaces induces aggregation of AuNPs.<sup>45</sup>

Based on the non-crosslinking aggregation mechanism, we recently developed a simple AuNP-based colorimetric assay for  $\text{Hg}^{2+}$ . AuNPs were firstly modified with the hydrophilic (11-mercaptopundecyl)trimethylammonium (MTA) terminated in positively charged quaternary ammonium groups (QA) to form QA-AuNPs, which were well-dispersed only in acidic aqueous solution due to the electrostatic repulsion between the QA cations and the positively charged hydrogen ions in media.<sup>46</sup> Upon the addition of  $\text{Hg}^{2+}$ , the extremely high affinity of thiolates toward  $\text{Hg}^{2+}$  triggered the breakage of Au–S bonds on the surfaces of AuNPs, causing QA-terminated thiols to dissociate from Au surfaces. The partial removal of ligands from the Au surfaces leads to the aggregation of AuNPs (Fig. 1A). Interestingly, since AuNPs may employ the photothermal effect to absorb photons to break the Au–S bond on the Au surface, we anticipated solar light irradiation could greatly improve the sensitivity of this assay *via* accelerating the displacement reaction of QA-AuNPs and  $\text{Hg}^{2+}$ . The limit of detection of this assay by the naked eye can be successfully decreased to as low as 30 nM (Fig. 1B, C), which is particularly attractive because the World Health Organization (WHO) has set a guideline value of  $\text{Hg}^{2+}$  in drinking water of  $0.006 \text{ mg L}^{-1}$  (30 nM), a value lower than the LOD of most currently available assays employing AuNPs. Therefore, we realized a simple colorimetric sensor for  $\text{Hg}^{2+}$  without resorting to any advanced instruments, and its selectivity and sensitivity is sufficient to monitor  $\text{Hg}^{2+}$  in drinking water. The practical potential of this assay was further evaluated in the real world by using simulated polluted samples.



Xingyu Jiang

*Xingyu Jiang is a Professor in the National Center for NanoScience and Technology of China (NCNST). His research interests include surface chemistry, microfluidics, micro/nano-fabrication, cell biology and immunoassays. He obtained his BS at The University of Chicago (1999), followed by an AM (2001) and a PhD (2004) from Harvard University (Chemistry), working with Professor George Whitesides. After a postdoctoral fellowship with Professor Whitesides, he joined NCNST in 2005.*

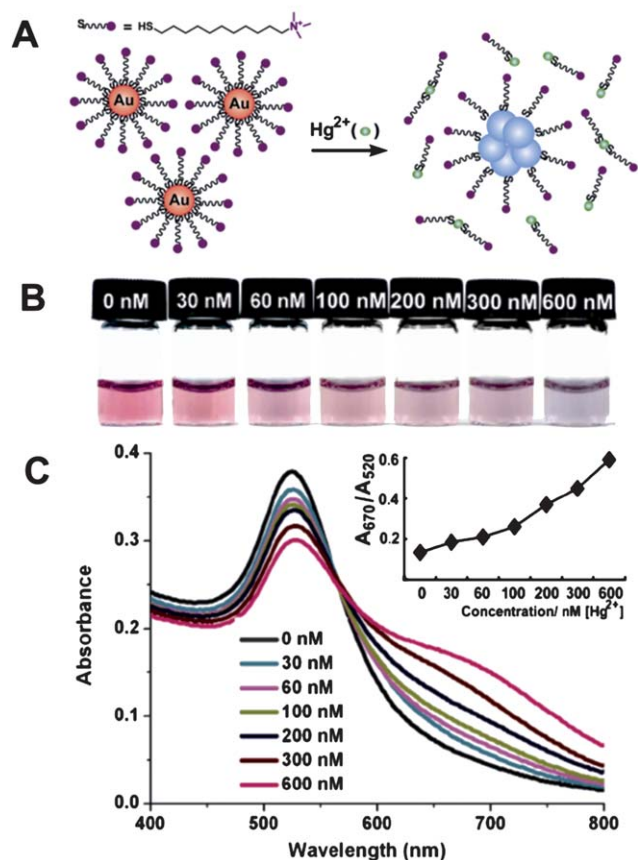


**Fig. 1** Colorimetric detection of  $\text{Hg}^{2+}$  based on the abstraction of quaternary ammonium group-terminated thiols from the surfaces of AuNPs. (A) The proposed mechanism for the  $\text{Hg}^{2+}$ -induced colorimetric response of QA-AuNPs. (B) Light irradiation-assisted detection of  $\text{Hg}^{2+}$  with the color change upon the increase of concentrations of  $\text{Hg}^{2+}$  from left to right. (C) Absorbance response for (B). Inset:  $A_{670}/A_{520}$  vs.  $\text{Hg}^{2+}$  concentrations. The irradiation time was 30 s, the pH value of the solutions was 1.0. Reproduced with permission from ref. 46. Copyright 2010, ACS.

Compared with the probes based on non-crosslinking aggregation mechanism, assays relying on the interparticle crosslinking aggregation mechanism have been increasingly explored. One classical interparticle crosslinking aggregation-based colorimetric assay for  $\text{Hg}^{2+}$  still relies on DNA-AuNPs. This simple platform for  $\text{Hg}^{2+}$  is dependent upon the binding of the T-T mismatches on the hybridized DNA-AuNPs with  $\text{Hg}^{2+}$  through interparticle T- $\text{Hg}^{2+}$ -T complex formation (Fig. 2),<sup>47,48</sup> which induces a more thermally stable DNA duplex that endows a higher melting temperature ( $T_m$ ) as compared with that in the absence of  $\text{Hg}^{2+}$ . This assay provides a LOD of 100 nM, which cannot satisfy the guideline value (30 nM) set by the WHO. Therefore, it is highly desirable to find a convenient colorimetric assay with sufficient sensitivity.

A chip-based scanometric assay with much higher sensitivity for  $\text{Hg}^{2+}$  has been provided to satisfy the guideline value set by the WHO. This method is based on the catalytic properties of the nanoparticles to reduce  $\text{Ag}^+$  as an amplification. The LOD of this assay is 10 nM for  $\text{Hg}^{2+}$  in buffer and natural samples

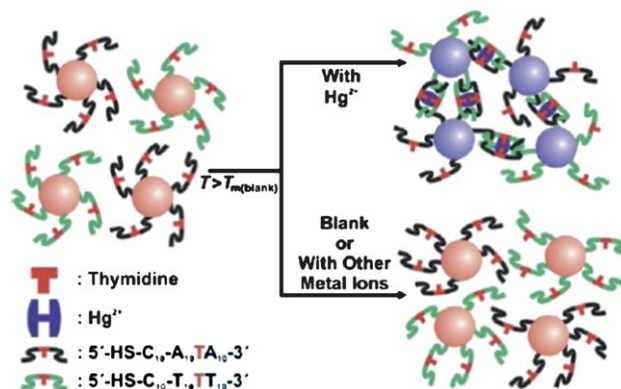


**Fig. 2** Colorimetric detection of  $\text{Hg}^{2+}$  based on DNA-modified AuNPs. Reproduced with permission from ref. 47. Copyright Wiley-VCH Verlag GmbH & Co.

(Fig. 3). This method is attractive for potential point-of-use applications due to its high throughput, convenient readout, and portability.<sup>49</sup> Importantly, to confirm the capacity of this method in the practical application, real samples from a lake were obtained and added with various concentrations of  $\text{Hg}^{2+}$ . The results fully agreed with those from ICP-MS.

Although DNA-AuNP-based methods are commonly sensitive, selective and simple, however, they require accurate control of temperature in this system to induce a visual color change. It is desirable to develop a detection system that is not only sensitive and selective, but also convenient and practical. Two types of non-complementary DNA-AuNPs probes and a specific single-stranded DNA sequence were designed to detect  $\text{Hg}^{2+}$  at room temperature. The single-stranded DNA is used as a linker that recognizes the two non-complementary sequences capped on surfaces of AuNPs. However, with the increasing number of T-T base-pair mismatches, the DNA-AuNPs cannot form aggregates in that the  $T_m$  of complementary DNA is lower than the operating temperature. As the researchers anticipated, a selected number of T-T base-pair mismatches would allow the hybridization of DNA-AuNPs at room temperature only in the presence of the  $\text{Hg}^{2+}$ .<sup>50</sup> This colorimetric assay that operates at room temperature makes DNA-AuNPs based sensor convenient in the real applications of detecting  $\text{Hg}^{2+}$ . Nevertheless, the as-reported LOD (1  $\mu\text{M}$ ) is much higher than the guideline value set by the WHO, a signal amplification method should be combined with this system.

Certain assays based on the formation of T- $\text{Hg}^{2+}$ -T complexes are promising to improve the simplicity and efficiency in real applications. For example, the use of fluorescence polarization assay (FPA) can significantly increase the sensitivity of the detection of  $\text{Hg}^{2+}$ . The LOD of this assay can reach as low as 1.0 nM.<sup>51</sup> Another crosslinking strategy for  $\text{Hg}^{2+}$  detection is in the formation of sulfur- $\text{Hg}^{2+}$ -sulfur (S- $\text{Hg}^{2+}$ -S) complex between different AuNPs, because  $\text{Hg}^{2+}$  exhibits much stronger thiophilic tendency than the competing heavy cations such as  $\text{Pb}^{2+}$ ,  $\text{Cd}^{2+}$ , and  $\text{Cu}^{2+}$ .<sup>52,53</sup>

Although the DNA-AuNP-based assays are promising tools for  $\text{Hg}^{2+}$  determination, DNA can be costly and difficult to handle. In addition, DNA-AuNP-based assays rely on accurate control of detection conditions.



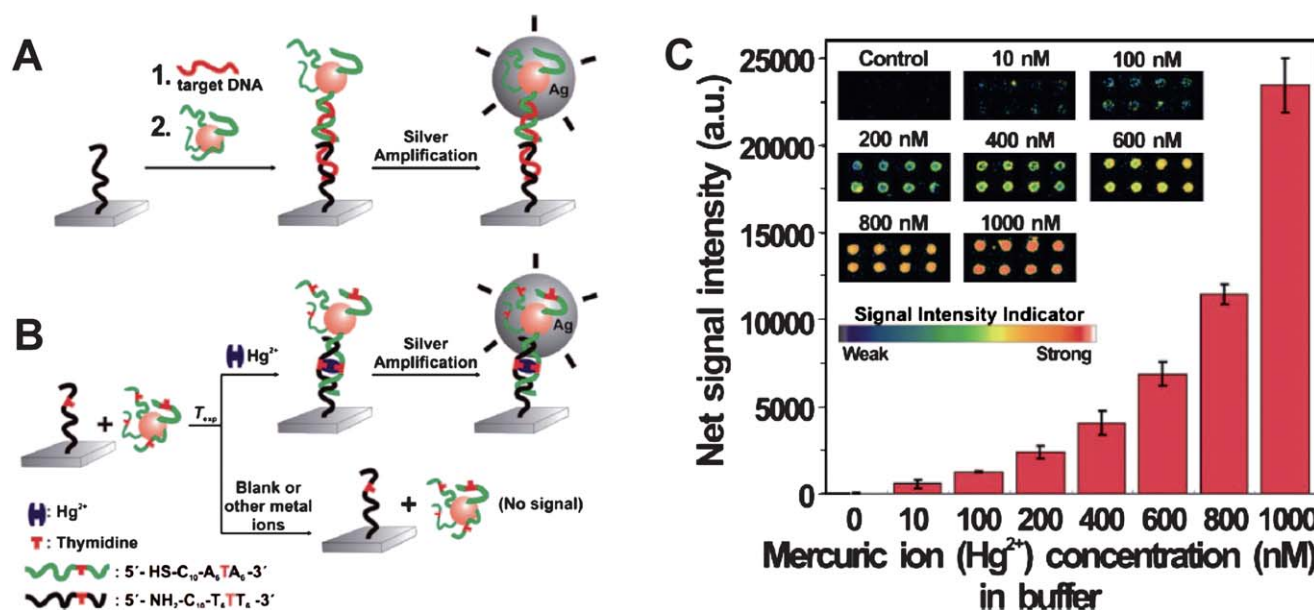


**Fig. 3** (A) Conventional chip-based scanometric detection of target DNA using DNA-AuNPs; and (B) chip-based scanometric detection of Hg<sup>2+</sup> using DNA-AuNPs. (C) Average scanometric signal intensity as a function of the Hg<sup>2+</sup> concentration in buffer. The corresponding scanometric signal images are shown as an inset. The spot diameter is ~200 μm. Reproduced with permission from ref. 49. Copyright 2008, ACS.

Another kind of simple colorimetric assay for Hg<sup>2+</sup> based on the interparticles crosslinking aggregation mechanism is carried out by using 3-mercaptopropionic acid (MPA)-functionalized AuNPs (MPA-AuNPs).<sup>54</sup> The ion-templated chelation between the acid groups on surfaces of AuNPs and Hg<sup>2+</sup> can induce the aggregation of AuNPs. Actually, the MPA-AuNPs lack sufficient selectivity for Hg<sup>2+</sup>, because metal ions such as Cd<sup>2+</sup> and Pb<sup>2+</sup> can readily interact with acid groups to cause the aggregation of MPA-AuNPs. To improve the selectivity, 2, 6-pyridinedicarboxylic acid (PDCA) must be added for masking Cd<sup>2+</sup> and Pb<sup>2+</sup>.<sup>55,56</sup>

Most reported colorimetric assays lack sufficient sensitivity for Hg<sup>2+</sup> determination. In order to enhance sensitivity, other technologies can combine with AuNPs. For example, hyper-Rayleigh scattering (HRS) can assist to improve the sensitivity of AuNP-based sensors modified with mercaptopropionic acid (MPA), homocysteine (HCys), and PDCA in the rapid and selective determination of Hg<sup>2+</sup> in tap water.<sup>57</sup> This approach has provided a high sensitivity (5 ppb). Another assay employs AuNP-based fluorescence resonance energy transfer (FRET) to screen mercury levels in contaminated soil, water, and fish with excellent sensitivity (2 ppt).<sup>58</sup> Recent advances have demonstrated the sensitivity for detecting Hg<sup>2+</sup> could even reach picomolar level by using localized surface plasmon resonance (LSPR).<sup>59</sup>

In general, assays based on fluorescence allow high sensitivity.<sup>60</sup> Ultra-small gold nanoparticles, often called gold nanoclusters (AuNCs), display strong fluorescence signals if the ligands capped on surfaces of AuNCs contain electron-rich groups.<sup>61</sup> Unlike colorimetric assays based on distance-dependant SPR absorption properties, fluorescent AuNCs (F-AuNCs) provide a promising perspective for bio-chemical analysis because they provide much lower LOD than colorimetric assays. AuNCs (2.9 ± 0.5 nm) capped by 11-mercaptopundecanoic acid

(MUA) (MUA-AuNCs) are used as a fluorescent probe that exhibits strong fluorescence signals. The ion-templated chelation between the acid groups and Hg<sup>2+</sup> can induce the aggregation of MUA-AuNCs, quenching the fluorescence of MUA-AuNCs. The LOD can be as low as 5.0 nM,<sup>62</sup> which is lower than the guideline value (30 nM) set by the WHO. The potential of this assay was evaluated in detecting environmental samples obtained from a pond, and the value was in good agreement with that determined by using ICP-MS. Another kind of fluorescent assay for Hg<sup>2+</sup> based on F-AuNCs has been reported owing to the fluorescence quenching of AuNCs caused by the specific and strong interactions between Hg<sup>2+</sup> and Au<sup>+</sup> on the gold surface, by which Hg<sup>2+</sup> can be detected with high sensitivity and selectivity.<sup>63–65</sup> For example, BSA-functionalized AuNCs (BSA-AuNCs) possess relatively high fluorescence (quantum yield ~ 6%), upon the addition of Hg<sup>2+</sup> into BSA-AuNCs solution, the fluorescence of AuNCs significantly diminished due to the metallophilic Hg<sup>2+</sup>–Au<sup>+</sup> interactions (Fig. 4).<sup>65</sup>

Another kind of AuNP-based assay relies on the quenching of the fluorescence of organic dyes by Au.<sup>66</sup> When Rhodamine 6G (R6G) adsorbs on the surfaces of AuNPs through noncovalent interactions, its fluorescence is efficiently quenched. Upon the addition of Hg<sup>2+</sup>, R6G are replaced from the surfaces of AuNPs to recover the intense fluorescence, which can be used to further detect Hg<sup>2+</sup>. The corresponding LOD can be as low as 6.0 × 10<sup>–11</sup> mol L<sup>–1</sup>. The recovered fluorescence intensity is proportional to the concentrations of Hg<sup>2+</sup>. This fluorescent assay has been successfully utilized in detecting real samples from tap water, pond water and river water. The values by using this method are consistent with those obtained by using atomic absorption spectroscopy.

In general, although many publications described various AuNP-based colorimetric and fluorescent methods in detecting Hg<sup>2+</sup>, most of them lacked sufficient sensitivity in monitoring

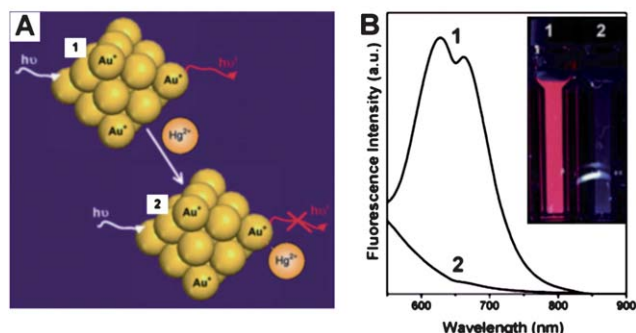


**Fig. 4** (A) Schematic of  $\text{Hg}^{2+}$  sensing based on the fluorescence quenching of AuNCs resulting from high-affinity metallophilic  $\text{Hg}^{2+}$ - $\text{Au}^+$  bonds. (b) Photoemission spectra ( $\lambda_{\text{ex}} = 470 \text{ nm}$ ) and (inset) photographs under UV light (354 nm) of AuNCs (20  $\mu\text{M}$ ) in the (1) absence and (2) presence of  $\text{Hg}^{2+}$  ions (50  $\mu\text{M}$ ). Reproduced with permission from ref. 65. Copyright 2009, RSC.

$\text{Hg}^{2+}$  in real samples. Furthermore, some of these assays show potential applications in environmental water and biological fluids, however most of them are limited to samples where  $\text{Hg}^{2+}$  is added to pure aqueous solutions. The primary obstacle for these assays is the interference from complicated components and high concentration of salt in environmental samples as well as biological fluids. Therefore, great effort is indispensable to develop more stable, reliable and accurate readout methods with sufficient sensitivity for  $\text{Hg}^{2+}$  in real samples.

## 2.2 Detection of copper ions

Copper is a transition metal essential for both plants and animals at certain concentrations, but it is toxic to living organisms at high concentrations.<sup>67</sup> The detection of copper is of great importance in food and biological samples.

Recently, our group provided a AuNP-based colorimetric method to detect  $\text{Cu}^{2+}$  ions by azide- and alkyne-functionalized AuNPs using click chemistry.<sup>68</sup> The catalyst of click chemistry,  $\text{Cu}^+$ , which can be quantitatively converted from the reduction of  $\text{Cu}^{2+}$  in the presence of sodium ascorbate which can in turn be used to conjugate the azide- and alkyne-functionalized AuNPs (Fig. 5A). The conjugation led to the aggregation of AuNPs along with the color change of the solution, and a precipitate eventually appeared after 24 h (Fig. 5B1). The procedure can be confirmed by UV-vis absorption spectrum. The absorption band red-shifted from 520 nm to about 580 nm, and the intensity decreased gradually (Fig. 5B2). This method allows the naked eye, without any advanced instrument, to detect  $\text{Cu}^{2+}$  with high selectivity over other metal ions. The LOD of the assay is 20  $\mu\text{M}$ , which is attractive because this value is the maximum contaminant level (MCL) for copper in drinking water defined by the US Environmental Protection Agency (EPA).<sup>69</sup>

One of the classical AuNP-based colorimetric probes for  $\text{Cu}^{2+}$  is based on  $\text{Cu}^{2+}$ -dependent DNA ligation DNAzyme, which can be catalyzed to form a phosphodiester bond in the presence of  $\text{Cu}^{2+}$ , thus, yielding a ligation product that is designed as a linker to assemble AuNPs, as a result, a red-to-blue color change is observed.<sup>70</sup>

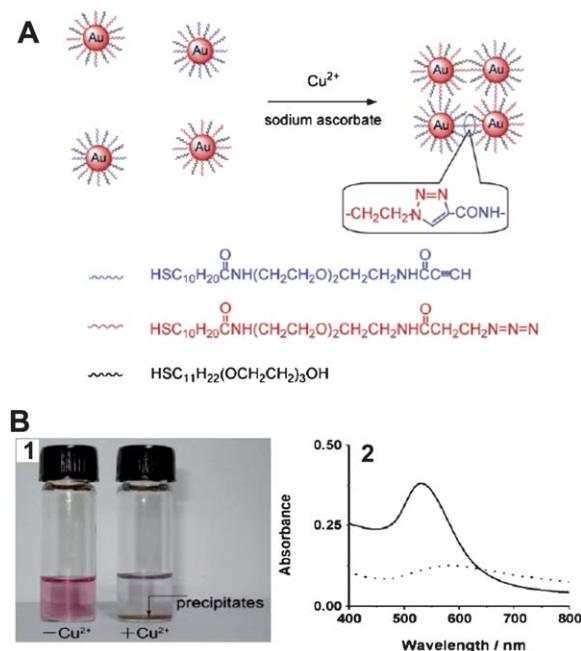


**Fig. 5** (A) The detection of  $\text{Cu}^{2+}$  ions using click chemistry between two types of AuNPs, each modified with thiols terminated in an alkyne or an azide functional group. (B) The assay for  $\text{Cu}^{2+}$  ions by the naked eye: (1) photographs of the solution containing only the mixture of functionalized AuNPs (left) and the same mixture after the addition of  $\text{Cu}^{2+}$  (right); (2) UV-vis spectrum obtained from solutions of functionalized AuNPs and after 24 h in the presence of  $\text{Cu}^{2+}$  ions and sodium ascorbate. Solid line: AuNPs- $\text{Cu}^{2+}$ ; dotted line: AuNPs +  $\text{Cu}^{2+}$ . Reproduced with permission from ref. 68. Copyright Wiley-VCH Verlag GmbH & Co.

Another interesting assay for  $\text{Cu}^{2+}$  is based on F-AuNPs, which has been functionalized with glutathione (GSH) that can interact with  $\text{Cu}^{2+}$  selectively to induce the aggregation of the GSH-capped F-AuNPs, accompanied by the decrease of the fluorescence intensity. The LOD is 3.6 nM, much lower than that from colorimetric assays.<sup>71</sup> Another work was based on fluorescence for detecting  $\text{Cu}^{2+}$  by using AuNPs as an ultra-efficient quencher. AuNPs were functionalized with the perylene bisimide chromophore (PBC) to form PBC-AuNPs by weak N-Au interactions, quenching the fluorescence of this chromophore. Upon the addition of  $\text{Cu}^{2+}$ , the chromophore was removed from the surfaces of AuNPs with fluorescence recovery owing to the stronger coordination ability of  $\text{Cu}^{2+}$  toward the pyridyl moiety in comparison with that of the AuNPs.<sup>72</sup>

The practical application of AuNP-based colorimetric assay has been demonstrated by using unmodified-AuNPs, which are easy to aggregate in high concentration of salt even in the presence of long  $\text{Cu}^{2+}$ -dependent DNAzyme. The addition of  $\text{Cu}^{2+}$  led to the self-cleave of the long DNAzyme into short pieces, which could absorb rapidly onto the unmodified-AuNPs to prevent the aggregation of AuNPs, thus the solution color remained red. Real samples from lake water were collected to further evaluate the availability of this colorimetric assay. The results were in a good agreement with those determined by using ICP-MS, demonstrating the capacity of this assay in detecting real samples.<sup>73</sup>

### 2.3 Detection of lead ions

Lead is one of the most toxic metallic pollutants to humans, especially to children.<sup>74</sup> The most classical AuNP-based assay for  $\text{Pb}^{2+}$  is based upon DNAzyme-directed assembly of AuNPs. Lu and his coworkers introduced such a kind of sensor for  $\text{Pb}^{2+}$  determination.<sup>75,76</sup> DNAzyme, known as one of the catalytically active DNA molecules, is easy to obtain and relatively stable. The structure of the  $\text{Pb}^{2+}$ -specific DNAzyme is shown in Fig. 6A. A typical DNAzyme is composed of a substrate strand (17DS) and an enzyme strand (17E), and the 17DS contains a single RNA linkage (ribonucleoside adenosine, rA) that can be hydrolytically cleaved in the presence of  $\text{Pb}^{2+}$  (Fig. 6B). To design the DNAzyme-based colorimetric sensor for  $\text{Pb}^{2+}$ , the 17DS has been extended on both the 3' and 5' ends for 12 bases, which is complementary to the 12-mer DNA attached on the surfaces of the 13-nm AuNPs. Through DNA hybridization, the extended substrate strand, 17E and 12-mer DNA-AuNPs can assemble to cause the aggregation of AuNPs and induce the red-to-blue color change. These aggregates can be used to detect  $\text{Pb}^{2+}$  by employing a heating-and-cooling process. If the aggregates are heated to above 50 °C ( $T_m = 46$  °C), and allowed to cool slowly to room temperature, the aggregates can be redispersed in the presence of  $\text{Pb}^{2+}$  due to the  $\text{Pb}^{2+}$ -caused cleavage of substrate strand in the process of cooling. If no  $\text{Pb}^{2+}$  is present, the reassembly of the three components can induce aggregation and shows a blue color (Fig. 6C). The required heating-and-cooling process takes about 2 h to observe the color change. The capacity of this assay for  $\text{Pb}^{2+}$  in real samples was evaluated by detecting and quantifying the contents of  $\text{Pb}^{2+}$  in leaded paints. To shorten

the responding time, the Lu group improved this system by using a “tail-to-tail” alignment and larger AuNPs, and the color change completed in less than 10 min at room temperature (Fig. 6D).<sup>77</sup> Although they improved this sensing system in various aspects, the detection limit of 100 nM is still higher than the MCL of 72 nM for lead in drinking water (by the EPA).<sup>78</sup>

Another piece of work is based on the phenomenon that single-stranded DNA can easily absorb onto AuNPs and prevent the salt-induced aggregation of AuNPs, while double-stranded DNA is stiffer and has negatively charged groups that repulse the interactions between double-stranded DNA and AuNPs, thus cannot prevent the salt-induced aggregation of AuNPs.<sup>79,80</sup> The  $\text{Pb}^{2+}$ -induced cleavage of DNAzyme releases single-stranded DNA from the surface of AuNPs to prevent the aggregation of AuNPs under high concentration of salt. By contrast, the absence of  $\text{Pb}^{2+}$  or the presence of other cations cannot prevent the formation of aggregates. This kind of assay, based on unmodified-AuNPs, has a LOD of 3 nM, which is much lower than the value defined by the EPA.<sup>81</sup> Based on the same principle, the authors transferred the DNAzyme-AuNPs into dipstick tests for the measurement of  $\text{Pb}^{2+}$ , and successfully demonstrated the validity of this sensor for the detection of  $\text{Pb}^{2+}$  in household leaded paints.<sup>82</sup>

Another kind of assay for  $\text{Pb}^{2+}$  is based on gallic acid-capped AuNPs (GA-AuNPs), on which  $\text{Pb}^{2+}$  can preferentially coordinate with phenolic hydroxyl groups of GA.<sup>83</sup> The LOD of GA-based probe was further improved to 10 nM by narrowing the size distribution of GA-AuNCs and minimizing interparticle repulsion between each GA-AuNC.<sup>84</sup> In addition, the feasibility of this GA-AuNC-based assay has been evaluated in seawater.

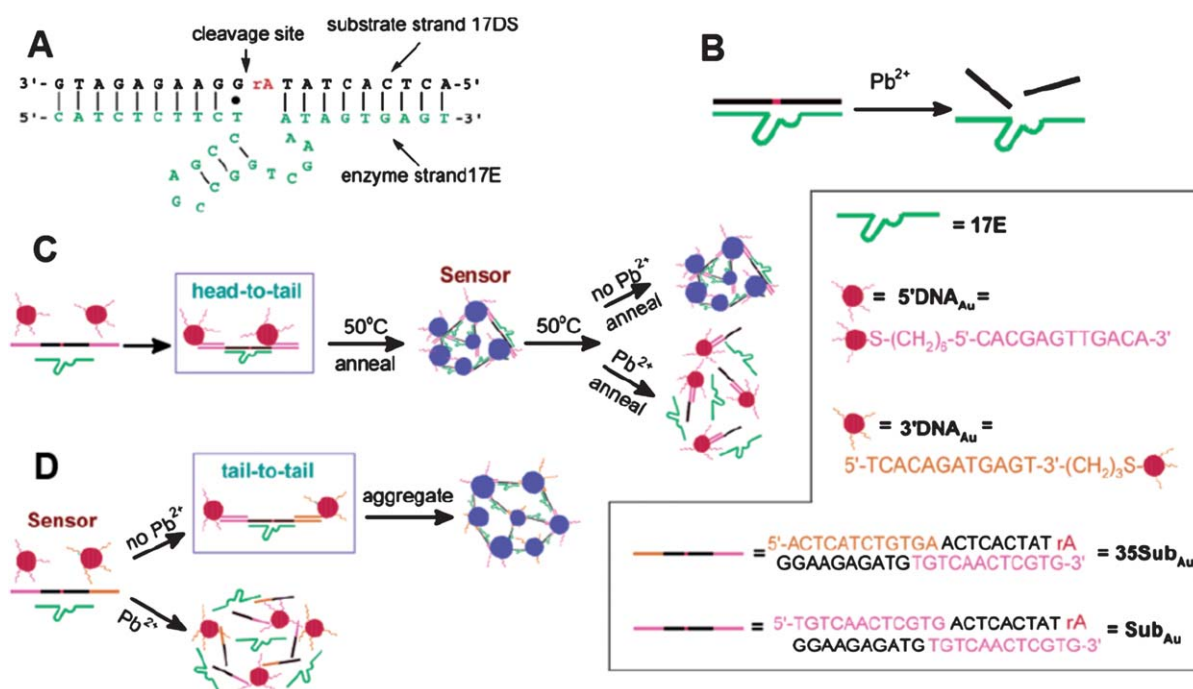


**Fig. 6** Colorimetric detection of  $\text{Pb}^{2+}$  based on DNAzyme modified AuNPs. (A) Secondary structure of the “8–17” DNAzyme. (B) Cleavage of 17DS by 17E in the presence of  $\text{Pb}^{2+}$ . (C) Schematics of the colorimetric  $\text{Pb}^{2+}$  sensor design. The three components (the extended substrate strand, 17E and 12-mer DNA-AuNPs) of the sensor can assemble to form blue-colored aggregates. Nanoparticles were aligned in a “head-to-tail” manner. A heating-and-cooling process (annealing) was needed for detection. (D) Schematics of the new colorimetric sensor design. Nanoparticles were aligned in a “tail-to-tail” manner. Reproduced with permission from ref. 77. Copyright 2004, ACS.



## 2.4 Detection of other cations

There are several AuNP-based colorimetric assays for some other important cations such as  $K^+$ ,<sup>85,86</sup>  $Cd^{2+}$ ,<sup>87</sup>  $As^{3+}$ ,<sup>88</sup>  $Ca^{2+}$ ,<sup>89,90</sup>  $Ag^+$ ,<sup>91</sup>  $Cr^{3+}$ ,<sup>92</sup> and  $Al^{3+}$ .<sup>93</sup> Arsenic contamination often threatens the safety of drinking water. An AuNP-based assay functionalized with GSH, dithiothreitol (DTT) and cysteine (Cys) has been reported for the determination of arsenic.<sup>88</sup> The stability constant between  $As^{3+}$  and the chelating ligands is much larger than other cations except for  $Hg^{2+}$ . By adding PDCA that can form much more stable complexes with  $Hg^{2+}$  than with other metal ions, the interference of  $Hg^{2+}$  can be strongly suppressed. With the help of dynamic light scattering (DLS), the LOD can be as low as 10 ppt, which is three orders of magnitude lower than the guideline value (10 ppb) that the WHO has set.<sup>94</sup>

The levels of  $Ca^{2+}$  are associated with several kinds of diseases,<sup>95</sup> thus accurate assays for  $Ca^{2+}$  are highly desirable. Calsequestrin (CSQ) is the most abundant calcium-binding protein and an endogenous  $Ca^{2+}$  ion sensor in the sarcoplasmic reticulum, so CSQ-functionalized AuNPs can be designed as a highly selective assay for  $Ca^{2+}$  determination.<sup>90</sup> The conformation of the CSQ molecules on surfaces of AuNPs can form dimers or polymers upon the addition of a threshold concentration of  $Ca^{2+}$ , thus results in the aggregation of AuNPs and a red-to-blue color change. Compared with most chemical chromophore-based  $Ca^{2+}$  ion sensors, this sensor is highly selective for  $Ca^{2+}$  over other divalent ions. This assay was used to detect  $Ca^{2+}$  in physiological samples, in which the contents of  $Ca^{2+}$  in normal and abnormal (hypocalcemic) conditions are different. After incubating these real samples with CSQ-functionalized AuNPs, the color of the solutions of abnormal condition changed from red to purple, and eventually a precipitate appeared, indicating the higher concentrations of  $Ca^{2+}$  in abnormal condition, while the color remained red for the normal condition of real samples. This tool is a classical AuNP-based sensor that used in the detection of physiologically related analytes, which is useful for monitoring certain diseases associated with high concentrations of  $Ca^{2+}$ .

We summarized the AuNP-based colorimetric and fluorescent assays for various cations in Table 1. From the overview of the AuNP-based assays for the detection of cations, we can perceive that the real samples are almost limited to the water-soluble samples, in which pretreatment is commonly required to remove other complicated components. So it is still difficult for AuNP-based systems to be used directly in complicated real samples owing to the instability of AuNPs, and more research is needed to focus on the improvement of the stability for AuNPs. Moreover, the uniform modification of AuNPs should be addressed, which is the key for the real sample applications based on AuNPs systems.

## 3. Assays for anions

Certain anions also act as severe pollutants to the environment and pose potentially adverse effects to human health.<sup>96–98</sup> It is desirable to develop a fast and accurate sensor to monitor toxic anions. The use of AuNPs as a colorimetric assay has a potential to construct convenient methods for detecting anions due to their SPR effect. Although AuNP-based colorimetric and fluorescent

assays have been widely used in detecting a variety of metallic ions, very little research has been devoted to the development of AuNP-based assays for anions.

The Griess reaction has been used to crosslink AuNPs and cause aggregation. This assay is based on the fact that sulfanilamide and naphthylethylenediamine can react to form an azo dye in the presence of nitrite ions ( $NO_2^-$ ) (Fig. 7A).<sup>99,100</sup> After preparing the “aniline AuNPs” and “naphthalene AuNPs” cofunctionalized with hydrophilic (11-mercaptopundecyl)-trimethylammonium (MTA), which enhances the solubility and stability of AuNPs in aqueous solutions (Fig. 7B), nitrite ions cause the cross-coupling of the two kinds of AuNPs *via* the Griess reaction.<sup>99</sup> As a result, the color of the solution changes from red to colorless (Fig. 7C). The MCL for nitrite ions in drinking water defined by the EPA is 1 ppm (21.7  $\mu M$ ),<sup>101</sup> a value similar to the LOD this assay presents (Fig. 7D). The capacity of this AuNP-based colorimetric assay was evaluated for the measurement of  $NO_2^-$  in environmental samples, such as lake water, and the results were similar to those in distilled water. Moreover, the products of  $NO_2^-$  derived from a reduction reaction were also monitored.

Another important kind of anion is cyanide ( $CN^-$ ), which has been extensively used in industry and has become a potential contaminant to ground water.<sup>102,103</sup> Cyanide can form stable complexes with transition metallic ions such as  $Cu^{2+}$  ions and abstract them from  $Cu^{2+}$  complexes to form new, more stable  $Cu^{2+}$ -cyanide complexes. Based on the fact, adenosine triphosphate-stabilized AuNPs (ATP-AuNPs) were designed to combine with  $Cu^{2+}$ -phenanthroline complexes. When exposed to cyanide,  $Cu^{2+}$ -phenanthroline can be decomplexed to release free phenanthroline, which can bind to Au surfaces accompanied with the removal of ATP from surfaces of AuNPs. Phenanthroline-coated AuNPs are unstable in aqueous media, thus lead to aggregation quickly along with a dramatic visible color change from red to blue of the solution.<sup>104</sup> The sensitivity of AuNP-based colorimetric assays for cyanide is generally insufficient for many settings. F-AuNPs is beneficial to improve the sensitivity for detecting cyanide. Most assays for cyanide based on F-AuNPs rely on the cyanide-induced etching of AuNPs,<sup>105,106</sup> in that cyanide can dissolve Au or Ag in water to form aqueous soluble metal–cyanide complex. By the addition of cyanide into solutions containing F-AuNPs that display molecule-like fluorescence,<sup>107</sup> the cyanide-based etching induces the decrease of the size of AuNCs, causing the fluorescence to decrease and even disappear completely. The highly reactive property of cyanide with inert Au endows this sensor superior selectivity over other common anions.

Some anions can be used as a negatively charged component in ionic liquids. In aqueous media, hydrophilic ionic liquid-coated AuNPs are mono-dispersed. When hydrophilic anions are replaced by hydrophobic species, the hydrophilic AuNPs aggregate, along with a color change of the solutions from red to blue. Based on this fact, hydrophobic anion such as  $PF_6^-$  can be detected by the naked eye by using methylimidazolium chloride-modified AuNPs (MC-AuNPs). The water soluble  $Cl^-$  species of ionic liquids on Au surfaces can be easily anion-exchanged by  $PF_6^-$  to form hydrophobic AuNPs, which are insoluble in aqueous media and thus lead to aggregation of AuNPs.<sup>108</sup> Hydrophilic fluoride ions ( $F^-$ ) can interact with phenylboronic

**Table 1** List of methods of colorimetric and fluorescent detection of cationic ions

Target	Probe	Readout	LOD/ $\mu\text{M}$	Real sample	Ref.
$\text{Hg}^{2+}$	DNA-AuNPs	Colorimetric/UV-vis	0.01	Underground water	45
	DNA-AuNPs	Colorimetric/UV-vis	0.1	—	47
	DNA-AuNPs	Colorimetric/Scanometric	0.01	Lake water	49
	DNA-AuNPs	Colorimetric/UV-vis	1.0	—	50
	QA-AuNPs	Colorimetric/UV-vis	0.03	Drinking water	46
	MPA-AuNPs	Colorimetric/UV-vis	0.1	—	54
	MUA-AuNCs	Colorimetric/UV-vis	$5.0 \times 10^{-3}$	Pond water	62
	Lysozyme-AuNCs	Fluorescence	0.01	—	63
	Lysozyme-AuNCs	Fluorescence	$3.0 \times 10^{-6}$	Seawater	64
	BSA-AuNCs	Fluorescence	$5.0 \times 10^{-4}$	—	65
	R6G-AuNPs	Fluorescence	$6.0 \times 10^{-5}$	River water	66
	Alkyne-AuNPs/Azide-AuNPs	Colorimetric/UV-vis	20.0	—	68
$\text{Cu}^{2+}$	DNA-AuNPs	Colorimetric/UV-vis	5.0	—	70
	GSH-AuNPs	Fluorescence	$3.6 \times 10^{-3}$	—	71
	PBC-AuNPs	Fluorescence	1.0	—	72
	DNA-AuNPs	Colorimetric/UV-vis	0.29	Lake water	73
$\text{Pb}^{2+}$	DNA-AuNPs	Colorimetric/UV-vis	0.1	Paint	77
	DNA-AuNPs	Colorimetric/UV-vis	$3.0 \times 10^{-3}$	Paint	82
	GA-AuNPs	Colorimetric/UV-vis	5.0	—	83
	GA-AuNCs	Fluorescence	0.01	Seawater	84
$\text{K}^{+}$	Citrate-AuNPs	Colorimetric/UV-vis	$1.0 \times 10^3$	—	85
	DNA-AuNPs	Fluorescence	—	—	86
$\text{As}^{3+}$	GSH/DTT/Cys-AuNPs	Colorimetric/UV-vis	$1.3 \times 10^{-4}$	Underground water	88
$\text{Ca}^{2+}$	CSQ-AuNPs	Colorimetric/UV-vis	$1.0 \times 10^3$	Human serum	90
$\text{Ag}^{+}$	DNA-AuNPs	Colorimetric/UV-vis	$5.9 \times 10^{-4}$	—	91
$\text{Cr}^{3+}$	DTNBA-AuNPs	Colorimetric/UV-vis	1.8	—	92
$\text{Al}^{3+}$	CALNN-AuNPs	Colorimetric/UV-vis	0.2	Cellular surface	93

acid under acidic conditions to form hydrophobic trifluoroborate anions ( $\text{Ar-BF}_3^-$ ). Similar to  $\text{PF}_6^-$ ,  $\text{Ar-BF}_3^-$  are hydrophobic species and can displace the hydrophilic anions originally absorbed on surfaces of AuNPs *via* an anion-exchange process. The formation of hydrophobic surface causes the aggregation AuNPs in aqueous media due to the hydrophobic interaction between different AuNPs.<sup>109</sup>

In addition, AuNP-embedded plasticized polymer membrane has been used to selectively recognize  $\text{I}^-$  by colorimetric sensing.<sup>110</sup> However, the detection limit of this assay is insufficient to determine  $\text{I}^-$  in the environmental and biological samples. The sensitivity for detecting  $\text{I}^-$  has been remarkably improved by using fluorescein isothiocyanate-capped AuNPs (FITC-AuNPs). The addition of  $\text{I}^-$  can remove FITC from Au surfaces accompanied with the release of the fluorescence of FITC, by which the total inorganic iodine ( $\text{I}^-$  and  $\text{IO}_3^-$ ) in edible salt and seawater have been determined as a practical application for this assay.<sup>111</sup> Similarly, colorimetric assays for oxoanions such as  $\text{AcO}^-$ ,  $\text{HPO}_4^{2-}$  and melonate in aqueous methanol by using isothiuronium-modified AuNPs have been reported.<sup>112</sup>

We summarized the AuNP-based colorimetric and fluorescent assays for various anions in Table 2. We noticed that even though more and more AuNP-based assays have been reported, it is still a challenge for the accurate determination of specific anions in aqueous media, because water soluble species surrounding the anionic analytes interfere with the desired interaction between anionic analytes and ligands on AuNPs, resulting in poor sensitivity and selectivity. Compared with ligands for cations, receptors for anions are more difficult to design, so AuNPs detection based on the surface modification still needs much work.

#### 4. Assays for small organic molecules

In recent years, a variety of AuNP-based assays have been developed to detect small organic molecules that play important roles in the human body, such as dopamine,<sup>113</sup> cocaine,<sup>114</sup> ATP,<sup>115,116</sup> glucose,<sup>117</sup> Cys,<sup>118–121</sup> and other biothiols (Table 3).<sup>122–124</sup> Dopamine, an important neurotransmitter of nervous systems, was monitored using unmodified AuNPs due to the hydrogen bonding interactions between the hydroxyl groups on dopamine that absorbed onto surfaces of unmodified AuNPs, thus leading to aggregation of AuNPs.<sup>113</sup> Based on unmodified AuNPs, the Fan group presented a novel design to detect ATP by using the anti-ATP aptamer, which possesses a highly selective affinity for ATP.<sup>115</sup> The anti-ATP aptamer exists in the form of a rigid duplex that cannot stabilize unmodified AuNPs in solution containing high concentrations of salt, while the presence of ATP can induce the formation of ssDNA, which binds to unmodified AuNPs and prevents the salt-induced aggregation. Based on the same principle, glucose existing in rat brain microdialysate has been monitored.<sup>117</sup> Most assays designed for compounds containing thiolate groups rely on their strong interaction with AuNPs *via* Au–S bonds, causing aggregation or redispersion of AuNPs along with a color change, which responds to the presence of specific biothiols. For example, fluorosurfactant (FSN) ligands, capped on surfaces of AuNPs as excellent stabilizing agents to disperse AuNPs in aqueous solutions even in the presence of high concentration of salt, can be displaced by Cys or HCys *via* the formation of Au–S bonds. The Cys or HCys-absorbed AuNPs are easy to aggregate mainly because of the electrostatic interaction and hydrogen bonding between the zwitterionic forms of amino acids on Au surfaces. None of other common amino acids can induce



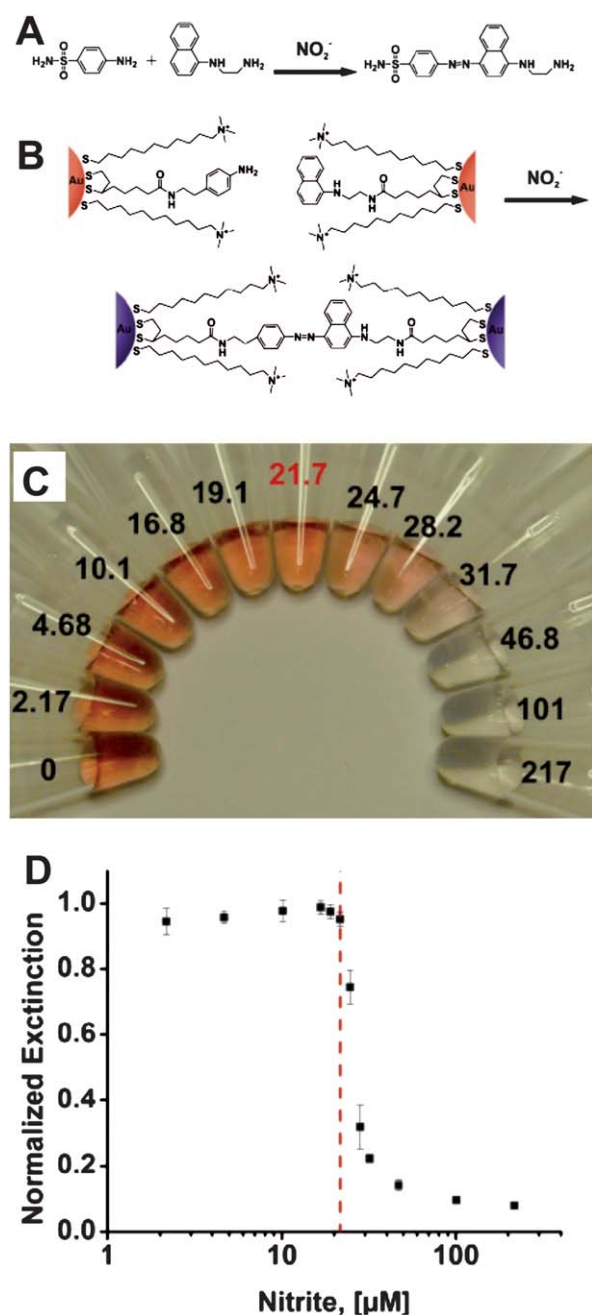


**Fig. 7** (A) Griess reaction. (B) Colorimetric detection of nitrite with functionalized AuNPs. (C) Photograph of particle solutions after incubation with various concentrations of nitrite. The nitrite concentrations, in  $\mu\text{M}$ , are listed next to the respective solutions. The MCL of nitrite in drinking water ( $21.7 \mu\text{M}$ ) is highlighted in red. (D) Particle solution extinction at 524 nm after incubation as a function of nitrite concentration. The red dashed line indicates the nitrite MCL. Reproduced with permission from ref. 99. Copyright 2009, ACS.

aggregation of FSN-AuNPs. The validity of this FSN-AuNP-based colorimetric assay has been demonstrated in monitoring the levels of Cys and Hcy in a human urine sample, indicating this method is promising for the detection of Cys and Hcy in biological fluids.<sup>125</sup> However, a lot more efforts such as changing the salt concentrations and particle size of FSN-AuNPs are needed to achieve the selectivity between Cys and HCys. More convenient

AuNP-based assays that can distinguish Cys and HCys in real samples are in high demand.

Based on FSN-AuNPs, the Tseng group developed two assays that can selectively detect Cys and HCys.<sup>121,126</sup> One is based on the fact that HCys can form a five-membered ring under the pretreatment of NaOH, which decreases the rate of HCys-induced removal of FSN ligands from surfaces of AuNPs, thereby slowing down the aggregation of FSN-AuNPs, but it is difficult for Cys to form a four-membered ring transition state under the same condition. Therefore, by pretreatment of aminothiols with NaOH, only Cys can remarkably induce the FSN-AuNPs aggregate.<sup>121</sup> Another FSN-AuNP-based assay has been successfully achieved for the selective detection of HCys. This method is based on the combination of several components including FSN-AuNPs, *o*-phthalaldehyde (OPA), as well as 2-mercaptoethanol (2-ME). FSN-AuNPs are used to abstract Cys and HCys, which can be easily removed from Au surfaces by 2-ME *via* ligand exchange. The released free HCys form complexes with OPA/2-ME and emit strong fluorescence, while the derivatization of Cys with OPA/2-ME displays extremely weak fluorescence. By comparing the finally resulted fluorescence, HCys are detected with good sensitivity as well as selectivity. The main drawback of this assay the requirement for a complex procedure.<sup>126</sup>

Some other organic small compounds show significant threat to both human beings and the environment, such as trinitrotoluene (TNT), which is most commonly used as an explosive for landmines.<sup>127</sup> Therefore, ultrasensitive assays for TNT have been increasingly developed in the past decade.<sup>128,129</sup> Mao *et al.* reported an excellent AuNP-based sensor for TNT. This sensor relied on the donor-acceptor (D-A) interaction between TNT and primary amines that modified AuNPs. The strong D-A interaction not only induced a direct colorimetric visualization for TNT, but also enabled this sensor to have a picomolar level of sensitivity.<sup>130</sup> By combining with SERS, Ray presented an accurate and fast probe to determine TNT.<sup>131</sup> In the presence of TNT, the Cys-modified AuNPs can form Meisenheimer complex with TNT *via* electrostatic interactions, thus can undergo aggregation, by which several hot spots formed and provided a significant enhancement of the sensitivity for TNT in aqueous solution with excellent selectivity.

Due to its harm to human health and its potential presence in dairy products, melamine has become a heated target for many types of assays.<sup>132–135</sup> Melamine itself contains several primary amine groups that can strongly bind with Au, thus readily displaces stabilizing agents (citrate)s from surfaces of AuNPs and causes the aggregation of AuNPs.<sup>136,137</sup> However, these unmodified AuNP-based assays cannot provide sufficient sensitivity for melamine determination. So the use of ligand-functionalized AuNPs is still a better choice to detect melamine.<sup>138</sup> Recently, Lu and his coworkers provided a simple but effective colorimetric assay with high sensitivity to detect melamine.<sup>139</sup> The working mechanism is based on the specific triple hydrogen-bonding recognition between melamine and a cyanuric acid (AC) derivatively functionalized on the surfaces of AuNPs (Fig. 8). The formation of the stable melamine-AC complex can lead to the aggregation of AC-modified AuNPs, along with a color change from red to blue just within 1 min even the concentration of melamine is as low as 2.5 ppb. Although the authors demonstrated the availability of this AuNP-based colorimetric assay in

**Table 2** List of methods of colorimetric and fluorescent detection of anions

Target	Probe	Readout	LOD/ $\mu\text{M}$	Real sample	Ref.
$\text{NO}_2^-$	Aniline-AuNPs/naphthalene-AuNPs	Colorimetric/UV-vis	22	Lake water	99
$\text{CN}^-$	ATP-AuNPs	Colorimetric/UV-vis	14	—	104
	RB-Au NPs	Fluorescence	0.08	—	105
	BSA-AuNCs	Fluorescence	0.2	Lake water	106
$\text{PF}_6^-$	MC-AuNPs	Colorimetric/UV-vis	—	—	108
$\text{F}^-$	Isothiuronium-AuNPs	Colorimetric/UV-vis	$8.0 \times 10^4$	—	109
$\text{I}^-$	FITC-AuNPs	Fluorescence	0.01	—	111
Oxoanions	Isothiuronium-AuNPs	Colorimetric/UV-vis	100	—	112

**Table 3** List of methods of colorimetric detection of small organic molecules

Target	Probe	Readout	LOD/ $\mu\text{M}$	Real sample	Ref.
Cys /HCys	FSN-AuNPs	Colorimetric/UV-vis	0.8	Human urine	125
Cys	FSN-AuNPs	Colorimetric/UV-vis	1.0	Human urine	121
HCys	FSN-AuNPs	Colorimetric/UV-vis	0.18	Human urine	126
TNT	Cysteamine-AuNPs	Colorimetric/UV-vis	$5.0 \times 10^{-7}$	Lake water	130
	Cys-AuNPs	Colorimetric/UV-vis/SERS	$2.0 \times 10^{-6}$	—	131
Melamine	Citrate-AuNPs	Colorimetric/UV-vis	0.32	Milk	136
	Citrate-AuNPs	Colorimetric/UV-vis	0.2	Milk	137
	PolyT <sub>n</sub> -AuNPs	Colorimetric/UV-vis	0.02	Milk	138
	MTT-AuNPs	Colorimetric/UV-vis	0.02	Milk	139
	Citrate-AuNPs	Colorimetric/UV-vis	20	—	114
Cocaine	DNA-AuNPs	Colorimetric/UV-vis	50	—	140
	Citrate-AuNPs	Colorimetric/UV-vis	0.03	—	113
Dopamine	Citrate-AuNPs	Colorimetric/UV-vis	0.6	—	115
ATP	CTAB-AuNPs	Colorimetric/UV-vis	200	—	116
Glucose	Citrate-AuNPs	Colorimetric/UV-vis	$1.0 \times 10^3$	Rat brain microdialysate	117

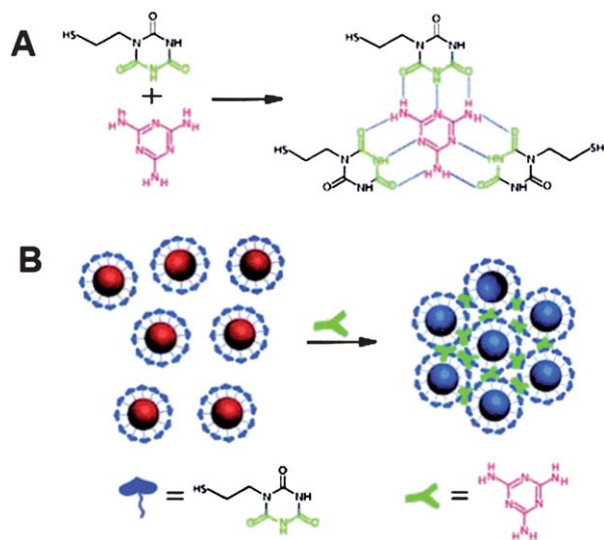


**Fig. 8** (A) Hydrogen-bonding recognition between melamine and cyanuric acid derivative. (B) Colorimetric detection of melamine using the cyanuric acid-stabilized AuNPs. Reproduced with permission from ref. 139. Copyright 2009, ACS.

detecting melamine in real samples such as raw milk as well as commercially available infant formula, it is time-consuming and a complicated pretreatment of real samples to remove the interference components was required. Therefore, more convenient AuNP-based colorimetric assays are still in high demand.

Fan and his coworkers provided a novel design to visually detect cocaine with high sensitivity by unmodified AuNPs and engineered aptamers. An anticocaine aptamer was firstly cut into two flexible ssDNA pieces, which can be assembled in the presence of cocaine. In previous discussions, we stated that unmodified AuNPs were easy to aggregate in aqueous solution with high concentrations of salt, while ssDNA-coated AuNPs were well-dispersed even at higher concentrations of salt. Therefore, the specific interaction between the pieces of aptamer and cocaine decreased the content of ssDNA, thus led to the aggregation of AuNPs in solution containing high concentrations of salt.<sup>114</sup> SsDNA aptamers can be designed to selectively interact with cocaine so that the structure of ssDNA aptamers changed, subsequently the hybridized bases that induced the aggregation of AuNPs decreased to several pairs, which were unstable at room temperature. The dehybridization of ssDNA aptamers thereby resulted in the redispersion of the aggregates of AuNPs.<sup>140</sup>

## 5. Conclusion and outlook

The colorimetric assays, which are easily visible to human eyes for the determination of the presence of targeted analytes, are desirable in most situations especially underdeveloped areas, where there is a lack of advanced instruments, or even electricity. Indeed, so far several drawbacks have limited the wide application of AuNP-based colorimetric assays in real samples. First, most functionalized AuNPs for specified targets are unstable in biological complex fluids like blood, urine, serum, and

environmental samples such as river water, lake water and sea water *etc.*, because the high concentrations of salt in these fluids cause different levels of aggregation of AuNPs. Second, some special components such as human serum albumin (HSA) in plasma are the most important interference for many AuNP-based assays in the practical applications. Third, a novel design and functionality of AuNPs for selective capture of target analytes needs a great deal of effort. Last, but not least, the sensitivity of AuNP-based colorimetric assays is generally insufficient for the detection of many targeted analytes in the real world. In order to enhance the sensitivity, the very rapidly developing AuNP-based fluorescent probes, including AuNCs and fluorescent molecules that are quenched by AuNPs *via* FRET, have been designed for targeted analytes. The fluorescence quantum yields of AuNCs are still much lower than most inorganic NCs or fluorescent molecules, and the practical applications of AuNCs for detecting targeted species need further demonstration. With respect to the “turn off” or “turn on” of the fluorescence of molecules that are quenched or recovered by AuNPs, time-consuming functionalization of fluorescent molecule on Au surface is generally required. Therefore, we think that even though AuNP-based colorimetric and fluorescent assays have a variety of advantages over most conventional tools with respect to simplicity, rapidity and cheapness, more efforts are still needed to improve the sensitivity, selectivity and availability. In particular, the practical applications of AuNP-based colorimetric and fluorescent assays in real samples are in high demand. By combining with different platforms such as fluorescence, DLS, SERS, HRS *etc.*, we hope that AuNP-based assays will be useful for many settings, including assays based on the solid substrate and lab-on-chip format, where highly sensitive assays requiring no advanced instrumentation are highly desired.<sup>141–144</sup>

## Acknowledgements

We thank the Chinese Academy of Sciences, the National Science Foundation of China (90813032, 20890020, 21025520), and the Ministry of Science and Technology (2009CB30001, 2011CB933201), the Chinese Academy of Sciences (KJCX2-YW-M15).

## References

- M. Wang, G. X. Zhang, D. Q. Zhang, D. B. Zhu and B. Z. Tang, *J. Mater. Chem.*, 2010, **20**, 1858–1867.
- E. M. Nolan and S. J. Lippard, *Chem. Rev.*, 2008, **108**, 3443–3480.
- L. Prodi, C. Bargossi, M. Montalti, N. Zaccheroni, N. Su, J. S. Bradshaw, R. M. Izatt and P. B. Savage, *J. Am. Chem. Soc.*, 2000, **122**, 6769–6770.
- B. C. Yin, B. C. Ye, W. H. Tan, H. Wang and C. C. Xie, *J. Am. Chem. Soc.*, 2009, **131**, 14624–14625.
- J. W. Liu, A. K. Brown, X. L. Meng, D. M. Crokek, J. D. Istok, D. B. Watson and Y. Lu, *Proc. Natl. Acad. Sci. U. S. A.*, 2007, **104**, 2056–2061.
- P. Chen and C. He, *J. Am. Chem. Soc.*, 2004, **126**, 728–729.
- K. Z. Brainina, N. Y. Stozhko and Z. V. Shalygina, *J. Anal. Chem.*, 2002, **57**, 945–949.
- E. Palomares, R. Vilar and J. R. Durrant, *Chem. Commun.*, 2004, 362–363.
- I. B. Kim and U. H. F. Bunz, *J. Am. Chem. Soc.*, 2006, **128**, 2818–2819.
- S. E. Cooper and B. J. Venton, *Anal. Bioanal. Chem.*, 2009, **394**, 329–336.
- C. Pöhlmann and M. Sprinzl, *Anal. Chem.*, 2010, **82**, 4434–4440.
- T. V. Barkhimer, J. R. Kirchhoff, R. A. Hudson, W. S. Messer and L. M. V. Tillekeratne, *Anal. Bioanal. Chem.*, 2008, **392**, 651–662.
- C. F. Ding, Q. Zhang and S. S. Zhang, *Biosens. Bioelectron.*, 2009, **24**, 2434–2440.
- K. C. Hu, D. X. Lan, X. M. Li and S. S. Zhang, *Anal. Chem.*, 2008, **80**, 9124–9130.
- C. M. Gikunju, S. M. Lev, A. Birenzige and D. M. Schaefer, *Talanta*, 2004, **62**, 741–744.
- Y. Liu, P. Liang and L. Guo, *Talanta*, 2005, **68**, 25–30.
- S. P. Wang, E. S. Forzani and N. J. Tao, *Anal. Chem.*, 2007, **79**, 4427–4432.
- T. Kang, S. Hong, J. Moon, S. Oh and J. Yi, *Chem. Commun.*, 2005, 3721–3723.
- E. Kopysc, K. Pyrzynska, S. Garbos and E. Bulska, *Anal. Sci.*, 2000, **16**, 1309–1312.
- K. A. Willets, *Anal. Bioanal. Chem.*, 2009, **394**, 85–94.
- M. D. Porter, R. J. Lipert, L. M. Siperko, G. Wang and R. Narayanan, *Chem. Soc. Rev.*, 2008, **37**, 1001–1011.
- C. M. Welch and R. G. Compton, *Anal. Bioanal. Chem.*, 2006, **384**, 601–619.
- S. Guo and E. Wang, *Anal. Chim. Acta*, 2007, **598**, 181–192.
- G. K. Vertelov, A. Y. Olenin and G. V. Lisichkin, *J. Anal. Chem.*, 2007, **62**, 813–824.
- S. Guo and S. Dong, *TrAC, Trends Anal. Chem.*, 2009, **28**, 96–109.
- R. Elghania, J. J. Storhoff, R. C. Mucic, R. L. Letsinger and C. A. Mirkin, *Science*, 1997, **277**, 1078–1081.
- C. C. You, O. R. Miranda, B. Gider, P. S. Ghosh, I. B. Kim, B. Erdogan, S. A. Krovi, U. H. F. Bunz and V. M. Rotello, *Nat. Nanotechnol.*, 2007, **2**, 318–323.
- R. Klajn, J. F. Stoddart and B. A. Grzybowski, *Chem. Soc. Rev.*, 2010, **39**, 2203–2237.
- S. K. Ghosh and T. Pal, *Chem. Rev.*, 2007, **107**, 4797–4862.
- M. C. Daniel and D. Astruc, *Chem. Rev.*, 2004, **104**, 293–346.
- W. Zhao, M. A. Brook and Y. Li, *ChemBioChem*, 2008, **9**, 2363–2371.
- Z. Wang and L. Ma, *Coord. Chem. Rev.*, 2009, **253**, 1607–1618.
- S. S. Agasti, S. Rana, M. H. Park, C. K. Kim, C. C. You and V. M. Rotello, *Adv. Drug Delivery Rev.*, 2010, **62**, 316–328.
- M. De, P. S. Ghosh and V. M. Rotello, *Adv. Mater.*, 2008, **20**, 4225–4241.
- R. A. Sperling, P. R. Gil, F. Zhang, M. Zanella and W. J. Parak, *Chem. Soc. Rev.*, 2008, **37**, 1896–1908.
- H. G. Park, *Biotechnol. Bioprocess Eng.*, 2003, **8**, 221–226.
- A. Renzoni, F. Zino and E. Franchi, *Environ. Res.*, 1998, **77**, 68–72.
- I. Onyido, A. R. Norris and E. Buncl, *Chem. Rev.*, 2004, **104**, 5911–5929.
- T. W. Clarkson, L. Magos and G. J. Myers, *N. Engl. J. Med.*, 2003, **349**, 1731–1737.
- F. M. M. Morel, A. M. L. Kraepiel and M. Amyot, *Annu. Rev. Ecol. Syst.*, 1998, **29**, 543–566.
- L. Li, B. X. Li, Y. Y. Qi and Y. Jin, *Anal. Bioanal. Chem.*, 2009, **393**, 2051–2057.
- X. W. Xu, J. Wang, K. Jiao and X. R. Yang, *Biosens. Bioelectron.*, 2009, **24**, 3153–3158.
- C. W. Liu, Y. T. Hsieh, C. C. Huang, Z. H. Lin and H. T. Chang, *Chem. Commun.*, 2008, 2242–2244.
- L. Wang, J. Zhang, X. Wang, Q. Huang, D. Pan, S. Song and C. Fan, *Gold Bull.*, 2008, **41**, 37–41.
- D. Li, A. Wieckowska and I. Willner, *Angew. Chem., Int. Ed.*, 2008, **47**, 3927–3931.
- D. B. Liu, W. S. Qu, W. W. Chen, W. Zhang, Z. Wang and X. Y. Jiang, *Anal. Chem.*, 2010, **82**, 9606–9610.
- J. S. Lee, M. S. Han and C. A. Mirkin, *Angew. Chem., Int. Ed.*, 2007, **46**, 4093–4096.
- S. He, D. Li, C. Zhu, S. Song, L. Wang, Y. Long and C. Fan, *Chem. Commun.*, 2008, 4885–4887.
- J. S. Lee and C. A. Mirkin, *Anal. Chem.*, 2008, **80**, 6805–6808.
- X. J. Xue, F. Wang and X. G. Liu, *J. Am. Chem. Soc.*, 2008, **130**, 3244–3245.
- B. C. Ye and B. C. Yin, *Angew. Chem., Int. Ed.*, 2008, **47**, 8386–8389.
- Y. R. Kim, R. K. Mahajan, J. S. Kim and H. Kim, *ACS Appl. Mater. Interfaces*, 2010, **2**, 292–295.
- Y. Fan, Y. F. Long and Y. F. Li, *Anal. Chim. Acta*, 2009, **653**, 207–211.
- C. C. Huang and H. T. Chang, *Chem. Commun.*, 2007, 1215–1217.



- 55 Z. Q. Tan, J. F. Liu, R. Liu, Y. G. Yin and G. B. Jiang, *Chem. Commun.*, 2009, 7030–7032.
- 56 Y. Wang, F. Yang and X. R. Yang, *Biosens. Bioelectron.*, 2010, **25**, 1994–1998.
- 57 G. K. Darbha, A. K. Singh, U. S. Rai, E. Yu, H. Yu and P. C. Ray, *J. Am. Chem. Soc.*, 2008, **130**, 8038–8043.
- 58 G. K. Darbha, A. Ray and P. C. Ray, *ACS Nano*, 2007, **1**, 208–214.
- 59 H. D. Song, I. Choi, Y. I. Yang, S. Hong, S. S. Lee, T. Kang and J. Yi, *Nanotechnology*, 2010, **21**, 145501.
- 60 C. W. Liu, C. C. Huang and H. T. Chang, *Langmuir*, 2008, **24**, 8346–8350.
- 61 Z. Wu, C. Gayathri, R. R. Gil and R. Jin, *J. Am. Chem. Soc.*, 2009, **131**, 6535–6542.
- 62 C. C. Huang, Z. Yang, H. K. Lee and H. T. Chang, *Angew. Chem., Int. Ed.*, 2007, **46**, 6824–6828.
- 63 H. Wei, Z. Wang, L. Yang, S. Tian, C. Hou and Y. Lu, *Analyst*, 2010, **135**, 1406–1410.
- 64 Y. H. Lin and W. L. Tseng, *Anal. Chem.*, 2010, **82**, 9194–9200.
- 65 J. Xie, Y. Zheng and J. Y. Ying, *Chem. Commun.*, 2010, **46**, 961–963.
- 66 J. L. Chen, A. F. Zheng, A. H. Chen, Y. C. Gao, C. Y. He, X. M. Kai, G. H. Wu and Y. C. Chen, *Anal. Chim. Acta*, 2007, **599**, 134–142.
- 67 E. Merian, *Metals and Their Compounds in the Environment*, VCH, Weinheim, 1991.
- 68 Y. Zhou, S. X. Wang, K. Zhang and X. Y. Jiang, *Angew. Chem., Int. Ed.*, 2008, **47**, 7454–7456.
- 69 X. Y. Xu, W. L. Daniel, W. Wei and C. A. Mirkin, *Small*, 2010, **6**, 623–626.
- 70 J. W. Liu and Y. Lu, *Chem. Commun.*, 2007, 4872–4874.
- 71 W. B. Chen, X. J. Tu and X. Q. Guo, *Chem. Commun.*, 2009, 1736–1738.
- 72 X. R. He, H. B. Liu, Y. L. Li, S. Wang, Y. J. Li, N. Wang, J. C. Xiao, X. H. Xu and D. B. Zhu, *Adv. Mater.*, 2005, **17**, 2811–2815.
- 73 Y. Wang, F. Yang and X. Yang, *Nanotechnology*, 2010, **21**, 205502.
- 74 H. L. Needleman, *Human Lead Exposure*, CRC Press, Boca Raton, FL, 1992.
- 75 J. W. Liu and Y. Lu, *J. Am. Chem. Soc.*, 2003, **125**, 6642–6643.
- 76 J. W. Liu and Y. Lu, *Chem. Mater.*, 2004, **16**, 3231–3238.
- 77 J. W. Liu and Y. Lu, *J. Am. Chem. Soc.*, 2004, **126**, 12298–12305.
- 78 <http://www.epa.gov/safewater/contaminants/index.html>.
- 79 H. X. Li and L. J. Rothberg, *J. Am. Chem. Soc.*, 2004, **126**, 10958–10961.
- 80 H. Wei, B. L. Li, J. Li, S. J. Dong and E. K. Wang, *Nanotechnology*, 2008, **19**, 095501.
- 81 Z. D. Wang, J. H. Lee and Y. Lu, *Adv. Mater.*, 2008, **20**, 3263–3267.
- 82 D. Mazumdar, J. W. Liu, G. Lu, J. Z. Zhou and Y. Lu, *Chem. Commun.*, 2010, **46**, 1416–1418.
- 83 K. Y. Saif, B. I. Ipe, C. H. Suresh and K. G. Thomas, *J. Phys. Chem. C*, 2007, **111**, 12839–12847.
- 84 K. W. Huang, C. J. Yua and W. L. Tseng, *Biosens. Bioelectron.*, 2010, **25**, 984–989.
- 85 L. Wang, X. Liu, X. Hu, S. Song and C. Fan, *Chem. Commun.*, 2006, 3780–3782.
- 86 J. Zhang, L. Wang, H. Zhang, F. Boey, S. Song and C. Fan, *Small*, 2010, **6**, 201–204.
- 87 Y. Kim, R. C. Johnson and J. T. Hupp, *Nano Lett.*, 2001, **1**, 165–167.
- 88 J. R. Kalluri, T. Arbneshi, S. A. Khan, A. Neely, P. Candice, B. Varisli, M. Washington, S. McAfee, B. Robinson, S. Banerjee, A. K. Singh, D. Senapati and P. C. Ray, *Angew. Chem., Int. Ed.*, 2009, **48**, 9668–9671.
- 89 A. J. Reynolds, A. H. Haines and D. A. Russell, *Langmuir*, 2006, **22**, 1156–1163.
- 90 S. Kim, J. W. Park, D. Kim, I. H. Lee and S. Jon, *Angew. Chem., Int. Ed.*, 2009, **48**, 4138–4141.
- 91 B. L. Li, Y. Du and S. J. Dong, *Anal. Chim. Acta*, 2009, **644**, 78–82.
- 92 Y. Q. Dang, H. W. Li, B. Wang, L. Li and Y. Q. Wu, *ACS Appl. Mater. Interfaces*, 2009, **1**, 1533–1538.
- 93 X. K. Li, J. Wang, L. L. Sun and Z. X. Wang, *Chem. Commun.*, 2010, **46**, 988–990.
- 94 <http://www.who.int/int-fs/en/fact210.html>.
- 95 M. M. Shepard and J. W. Smith, *Am. J. Med. Sci.*, 2007, **334**, 381–385.
- 96 M. Boiocchi, L. D. Boca, D. E. Gomez, L. Fabbri, M. Licchelli and E. Monzani, *J. Am. Chem. Soc.*, 2004, **126**, 16507–16514.
- 97 P. D. Beer and P. A. Gale, *Angew. Chem., Int. Ed.*, 2001, **40**, 486–516.
- 98 J. D. Brender, J. M. Olive, M. Felkner, L. Suarez, W. Marckwardt and K. A. Hendricks, *Epidemiology*, 2004, **15**, 330–336.
- 99 W. L. Daniel, H. S. Han, J. S. Lee and C. A. Mirkin, *J. Am. Chem. Soc.*, 2009, **131**, 6362–6363.
- 100 B. S. Garg, Y. L. Mehta and M. Katyal, *Talanta*, 1976, **23**, 71–71.
- 101 M. J. Focazio, D. Tipton, S. D. Shapiro and L. H. Geiger, *Ground Water Monit. Remediation*, 2006, **26**, 92–104.
- 102 K. W. Kulig, *Cyanide Toxicity*, US Department of Health and Human Services, Atlanta, 1991.
- 103 B. Vennesland, E. E. Comm, C. J. Knowles, J. Westly and F. Wissing, *Cyanide in Biology*, Academic Press, London, 1981.
- 104 M. H. Kim, S. Kim, H. H. Jang, S. Yi, S. H. Seo and M. S. Han, *Tetrahedron Lett.*, 2010, **51**, 4712–4716.
- 105 L. Shang, L. H. Jin and S. J. Dong, *Chem. Commun.*, 2009, 3077–3079.
- 106 Y. L. Liu, K. L. Ai, X. L. Cheng, L. H. Huo and L. H. Lu, *Adv. Funct. Mater.*, 2010, **20**, 951–956.
- 107 J. P. Xie, Y. G. Zheng and J. Y. Ying, *J. Am. Chem. Soc.*, 2009, **131**, 888–889.
- 108 H. Itoh, K. Naka and Y. Chujo, *J. Am. Chem. Soc.*, 2004, **126**, 3026–3027.
- 109 T. Minami, K. Kaneko, T. Nagasaki and Y. Kubo, *Tetrahedron Lett.*, 2008, **49**, 432–436.
- 110 K. Y. Lee, D. W. Kim, J. Heo, J. S. Kim, J. K. Yang, G. W. Cheong and S. W. Han, *Bull. Korean Chem. Soc.*, 2006, **27**, 2081–2083.
- 111 Y. M. Chen, T. L. Cheng and W. L. Tseng, *Analyst*, 2009, **134**, 2106–2112.
- 112 Y. Kubo, S. Uchida, Y. Kemmochi and T. Okubo, *Tetrahedron Lett.*, 2005, **46**, 4369–4372.
- 113 Y. F. Zhang, B. X. Li and X. L. Chen, *Microchim. Acta*, 2009, **168**, 107–113.
- 114 J. Zhang, L. H. Wang, D. Pan, S. P. Song, F. Y. C. Boey, H. Zhang and C. H. Fan, *Small*, 2008, **4**, 1196–1200.
- 115 J. Wang, L. H. Wang, X. F. Liu, Z. Q. Liang, S. P. Song, W. X. Li, G. X. Li and C. H. Fan, *Adv. Mater.*, 2007, **19**, 3943–3946.
- 116 C. M. Li, Y. F. Li, J. Wang and C. Z. Huang, *Talanta*, 2010, **81**, 1339–1345.
- 117 Y. Jiang, H. Zhao, Y. Q. Lin, N. N. Zhu, Y. R. Ma and L. Q. Mao, *Angew. Chem., Int. Ed.*, 2010, **49**, 4800–4804.
- 118 Z. Chen, S. L. Luo, C. B. Liu and Q. Y. Cai, *Anal. Bioanal. Chem.*, 2009, **395**, 489–494.
- 119 J. S. Lee, P. A. Ulmann, M. S. Han and C. A. Mirkin, *Nano Lett.*, 2008, **8**, 529–533.
- 120 L. Shang, C. J. Qin, T. Wang, M. Wang, L. X. Wang and S. J. Dong, *J. Phys. Chem. C*, 2007, **111**, 13414–13417.
- 121 H. P. Wu, C. C. Huang, T. L. Cheng and W. L. Tseng, *Talanta*, 2008, **76**, 347–352.
- 122 S. Durocher, A. Rezaee, C. Hamm, C. Rangan, S. Mittler and B. Mutus, *J. Am. Chem. Soc.*, 2009, **131**, 2475–2477.
- 123 C. C. Huang and W. L. Tseng, *Anal. Chem.*, 2008, **80**, 6345–6350.
- 124 M. D. Li, T. L. Cheng and W. L. Tseng, *Electrophoresis*, 2009, **30**, 388–395.
- 125 C. Lu and Y. B. Zu, *Chem. Commun.*, 2007, 3871–3873.
- 126 J. H. Lin, C. W. Chang and W. L. Tseng, *Analyst*, 2010, **135**, 104–110.
- 127 J. Hawari, S. Beaudet, A. Halasz, S. Thiboutot and G. Ampleman, *Appl. Microbiol. Biotechnol.*, 2000, **54**, 605–618.
- 128 M. Riskin, R. Tel-Vered, T. Bourenko, E. Granot and I. Willner, *J. Am. Chem. Soc.*, 2008, **130**, 9726–9733.
- 129 M. Riskin, R. Tel-Vered, O. Lioubashevski and I. Willner, *J. Am. Chem. Soc.*, 2009, **131**, 7368–7378.
- 130 Y. Jiang, H. Zhao, N. N. Zhu, Y. Q. Lin, P. Yu and L. Q. Mao, *Angew. Chem., Int. Ed.*, 2008, **47**, 8601–8604.
- 131 S. S. R. Dasary, A. K. Singh, D. Senapati, H. Yu and P. C. Ray, *J. Am. Chem. Soc.*, 2009, **131**, 13806–13812.
- 132 S. P. Yang, J. H. Ding, J. Zheng, B. Hu, J. Q. Li, H. W. Chen, Z. Q. Zhou and X. L. Qiao, *Anal. Chem.*, 2009, **81**, 2426–2436.
- 133 Y. C. Tyan, M. H. Yang, S. B. Jong, C. K. Wang and J. Shiea, *Anal. Bioanal. Chem.*, 2009, **395**, 729–735.
- 134 L. Zhu, G. Gamez, H. W. Chen, K. Chinglin and R. Zenobi, *Chem. Commun.*, 2009, 559–561.
- 135 H. Zhu, S. X. Zhang, M. X. Li, Y. H. Shao and Z. W. Zhu, *Chem. Commun.*, 2010, **46**, 2259–2261.
- 136 F. Wei, R. Lam, S. Cheng, S. Lu, D. Ho and N. Li, *Appl. Phys. Lett.*, 2010, **96**, 133702.
- 137 H. Chi, B. H. Liu, G. J. Guan, Z. P. Zhang and M. Y. Han, *Analyst*, 2010, **135**, 1070–1075.

- 
- 138 W. J. Qi, D. Wu, J. Ling and C. Z. Huang, *Chem. Commun.*, 2010, **46**, 4893–4895.
- 139 K. L. Ai, Y. L. Liu and L. H. Lu, *J. Am. Chem. Soc.*, 2009, **131**, 9496–9497.
- 140 J. W. Liu and Y. Lu, *Angew. Chem., Int. Ed.*, 2006, **45**, 90–94.
- 141 Y. Y. Liu, D. Y. Yang, T. Yu and X. Y. Jiang, *Electrophoresis*, 2009, **30**, 3269–3275.
- 142 Y. Sun, Y. Y. Liu, W. S. Qu and X. Y. Jiang, *Anal. Chim. Acta*, 2009, **650**, 98–105.
- 143 D. Y. Yang, X. Niu, Y. Y. Liu, Y. Wang, X. Gu, L. S. Song, R. Zhao, L. Y. Ma, Y. M. Shao and X. Y. Jiang, *Adv. Mater.*, 2008, **20**, 4770–4775.
- 144 W. Zhang, S. Lin, C. Wang, J. Hu, C. Li, Z. Zhuang, Y. Zhou, R. A. Mathies and C. J. Yang, *Lab Chip*, 2009, **9**, 3088–3094.